COMBINATION OF DENSITY AND ENERGY MODULATION IN MICROBUNCHING ANALYSIS[*]

Cheng-Ying Tsai[#], Department of Physics, Virginia Tech, VA 24061, USA
Rui Li, Jefferson Lab, Newport News, VA 23606, USA

Abstract

Microbunching instability (MBI) has been one of the most challenging issues in the transport of high-brightness electron beams for modern recirculating or energy recovery linac machines. Recently we have developed and implemented a Vlasov solver [1] to calculate the microbunching gain for an arbitrary beamline lattice, based on the extension of existing theoretical formulation [2-4] for the microbunching amplification from an initial density perturbation to the final density modulation. For more thorough analyses, in addition to the case of (initial) density to (final) density amplification, we extend in this paper the previous formulation to more general cases, including energy to density, density to energy and energy to energy amplifications for a recirculation machine. Such semi-analytical formulae are then incorporated into our Vlasov solver, and qualitative agreement is obtained when the semi-analytical Vlasov results are compared with particle tracking simulation using ELEGANT [5].

INTRODUCTION

Theoretical formulation of MBI has been developed both in single-pass [2-4] and in storage-ring [6,7] systems. Hetfeis *et al.* [2] derived a linear integral equation in terms of the density modulation (or, the bunching factor). Huang and Kim [3] obtained the integral equation in a more compact way and outlined the microbunching due to initial energy modulation. This has become the building block for this work.

To quantify MBI in a general transport system, we estimate the microbunching amplification factor (or, gain) along the beamline. For a long transport line of a recirculation machine, people usually treat the microbunching problem as a single-pass system. More generally, concatenations of sub-beamline sections were treated and the overall microbunching gain is speculated as the multiplication of gains from individual subsections [3,8]. Though this concatenation approach seems intuitive, we need a more rigorous and detailed justification of the validity.

In this paper, we consider a more generalized situation where both initial density and energy modulations can be present and derive a set of integral equations for the microbunching evolution in terms of density and energy modulations along a general beamline. Then we study an example of recirculating beamline. From the simulation results, we have some interesting observations and have

found such combined analysis of density and energy modulation can give more information than the previous treatment. Comparison of the results with ELEGANT tracking has given qualitative agreement. Possible extension of this study to include transverse microbunching is underway.

THEORY

From the (linearized) Vlasov equation, the evolution of the phase-space distribution function is governed by [3]

$$f(X;s) = f_0(X_0) - \int_0^s d\tau \left(\frac{\partial f_0}{\partial \delta_\tau}\right)\left(\frac{\partial \delta}{\partial \tau}\right) \qquad (1)$$

where the energy change due to collective effect can be induced by density modulation

$$\frac{d\delta}{d\tau} = -\frac{Nr_e}{\gamma}\int \frac{dk_1}{2\pi} Z(k_1;\tau)b(k_1;\tau)e^{ik_1 z_\tau}. \qquad (2)$$

Here f is the beam phase-space distribution function, $X(s) = (x, x', z, \delta; s)$ the phase-space variables, N the number of particles, γ the Lorentz factor, $Z(k)$ the longitudinal impedance per unit length, k the modulation wavenumber, and $b(k)$ the density modulation.

We then defined two quantities for subsequent analysis:

$$b(k;s) = \frac{1}{N}\int dX\, f(X;s)e^{-ik_z(s)z_s} \qquad (3)$$

as the density modulation (or, bunching factor), and

$$p(k;s) = \frac{1}{N}\int dX(\delta_s)f(X;s)e^{-ik_z(s)z_s} \qquad (4)$$

as the energy modulation.

In the absence of collective effect, we have $f(X;s) = f_0(X_0)$, i.e. the distribution function can be completely determined by the initial distribution. Assume initial unperturbed phase-space distribution is of the form

$$\bar{f}_0(X_0) = \frac{n_0}{2\pi\varepsilon_0\sqrt{2\pi}\sigma_\delta}e^{-\frac{x_0^2+(\beta_0 x_0'+\alpha_0 x_0)^2}{2\varepsilon_0\beta_0}-\frac{\delta_0^2}{2\sigma_\delta^2}}, \qquad (5)$$

where n_0 is the line density, ε_0 and σ_δ are the emittance and energy spread of the beam, α_0 and β_0 are initial Twiss parameters. For simplicity, assume no chirp on the beam.

Equations (3) and (4) can be analytically obtained to be

$$b_0^d(k;s) = b_0(k_0;0)\{L.D;s\} \qquad (6)$$

as the density modulation due to initial density modulation in the absence of collective effect, where

$$\{L.D;s\} \equiv e^{-\frac{k_z^2(s)\varepsilon_0\beta_0}{2}\left(R_{51}(s)-\frac{\alpha_0}{\beta_0}R_{52}(s)\right)^2-\frac{k_z(s)\varepsilon_0}{2\beta_0}R_{52}^2(s)-\frac{k_z^2(s)\sigma_\delta^2}{2}R_{56}^2(s)} \qquad (7)$$

Here R_{5i} denote standard linear transport matrix elements.

Similarly, we have, in the absence of collective effect, $b_0^e(k;s)$ as density modulation due to initial energy modulation; $p_0^d(k;s)$ as energy modulation due to initial density modulation; $p_0^e(k;s)$ as energy modulation due to initial energy modulation.

In the presence of collective effect, the governing equation Eq. (1) can be re-written in terms of density or energy modulations:

$$b(k;s) = b_0(k;s) - \frac{ik_z(s)}{N}\int_0^s d\tau R_{56}(s' \to s)\int dX_\tau f_0(X_\tau)e^{-ik_z(s)z_s(X_\tau)}\left(\frac{d\delta}{d\tau}\right) \quad (8)$$

and

$$p(k;s) = p_0(k;s) - \frac{ik_z(s)}{N}\int_0^s d\tau R_{56}(s' \to s)\int dX_\tau(\delta_s)f_0(X_\tau)e^{-ik_z(s)z_s(X_\tau)}\left(\frac{d\delta}{d\tau}\right)$$
$$+ \frac{1}{N}\int_0^s d\tau\int dX_\tau f_0(X_\tau)e^{-ik_z(s)z_s(X_\tau)}\left(\frac{d\delta}{d\tau}\right) \quad (9)$$

After linearizing Eqs.(8) and (9) and neglecting higher order terms in the integration, we can obtain four integral equations. Since the integral equations are linear in $b(k;s)$ and $p(k;s)$, they can be cast into a vector-matrix notation,

$$\begin{bmatrix} \mathbf{b}^d \\ \mathbf{b}^e \\ \mathbf{p}^d \\ \mathbf{p}^e \end{bmatrix} = \underbrace{\begin{pmatrix} (1-\mathbf{K})^{-1} & 0 & 0 & 0 \\ 0 & (1-\mathbf{K})^{-1} & 0 & 0 \\ (\mathbf{M}-\mathbf{L})(1-\mathbf{K})^{-1} & 0 & 1 & 0 \\ 0 & (\mathbf{M}-\mathbf{L})(1-\mathbf{K})^{-1} & 0 & 1 \end{pmatrix}}_{\equiv \mathbf{T}}_{4M\times 4M} \begin{bmatrix} \mathbf{b}_0^d \\ \mathbf{b}_0^e \\ \mathbf{p}_0^d \\ \mathbf{p}_0^e \end{bmatrix}$$

where

$$\mathbf{K} \equiv ik_z(s)\frac{I(\tau)}{\gamma I_A}R_{56}(\tau \to s)Z(k(\tau);\tau)\{\text{L.D.};\tau,s\} \quad (10)$$

$$\mathbf{M} \equiv ik_z^2(s)\frac{I(\tau)}{\gamma I_A}\sigma_\delta^2 R_{56}(\tau \to s)U(s,\tau)Z(k(\tau);\tau)\{\text{L.D.};\tau,s\} \quad (11)$$

$$\mathbf{L} \equiv \frac{I(\tau)}{\gamma I_A}Z(k(\tau);\tau)\{\text{L.D.};\tau,s\} \quad (12)$$

Here $I(\tau)$ is the beam current at $s = \tau$, I_A is Alfven current,

$$\{\text{L.D.};\tau,s\} \equiv e^{-\frac{k_z^2(s)\varepsilon_0\beta_0}{2}\left(V(s,\tau)-\frac{\alpha_0}{\beta_0}W(s,\tau)\right)^2 - \frac{k_z(s)\varepsilon_0}{2\beta_0}W^2(s,\tau) - \frac{k_z^2(s)\sigma_\delta^2}{2}U^2(s,\tau)}$$

$U(s,\tau) = R_{56}(s)-R_{56}(\tau)$, $V(s,\tau) = R_{51}(s)-R_{51}(\tau)$, and $W(s,\tau) = R_{52}(s)-R_{52}(\tau)$.

The concept of microbunching gain can in general be extended to have the four combinations, $\left|b^d/b_0^d(0)\right|$, $\left|b^e/p_0^e(0)\right|$, $\left|p^d/b_0^d(0)\right|$, and $\left|p^e/p_0^d(0)\right|$, but hereafter we would use density and energy modulations $b(k;s)$ and $p(k;s)$ unless mentioned otherwise. It is worth mentioning that the matrix equation can be reduced to that in Ref. [9] for $O(\mathbf{K}) \ll 1$.

CONCATENATION OF BEAMLINE

In this section, we would apply the generalized formulation to an example of recirculating machine [10]. This recirculating beamline consists of two arcs, for which are based on the original design in Ref. [11]. One of the arcs is composed of 4 triple-bend-achromatic (TBA) units. The arcs are achromatic and quasi-isochronous. Let us separate this machine into four pieces: S1, ARC1, S2, and ARC2 (see Fig. 1). In this example, the beam is assumed 150 MeV in energy, peak bunch current 60 A, with normalized emittance 0.4 μm and relative energy spread 1.33×10^{-5}. Figure 2 shows Twiss and momentum compaction functions along the beamline. Below we would estimate both the density and

energy modulations at the end of the beamline but begin from different sub-beamline sections, and compare all of the obtained results from different concatenations. Let us consider the simplest case shown in Fig. 3, where the modulations evolve in the absence of collective effects (i.e. pure optics). The concatenations of the matrices **T** from sub-beamline sections match well with that of the start-to-end case, in our intuitive expectation. Now we include steady-state CSR [12,13], which only occurs in ARC1 and ARC2. Figure 4 shows the density and energy modulation spectra at the end of the beamline. From the figure, we can see differences between red/green and blue/black curves. We claim that the differences originate from *correlation* between ARC1 and ARC2. That is to say, for S2-ARC2 case, the initial conditions used in our analysis [*b*, *p*]$^\text{T}$, given at the exit of ARC1, are not sufficient to fully describe the CSR interaction occurred upstream in ARC1. To confirm, we artificially switch off the CSR in ARC1 (but retain the CSR in ARC2) and find all the spectra of density and energy modulations from different concatenations agree well, as shown in Fig. 5.
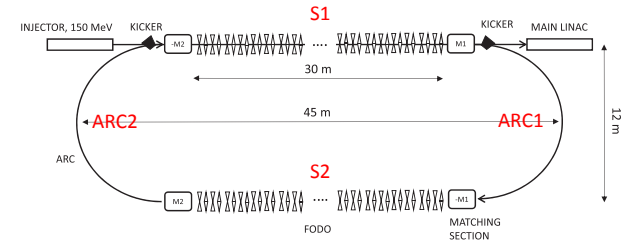

Figure 1: Schematic layout of the recirculating beamline (not to scale), from Ref. [10].
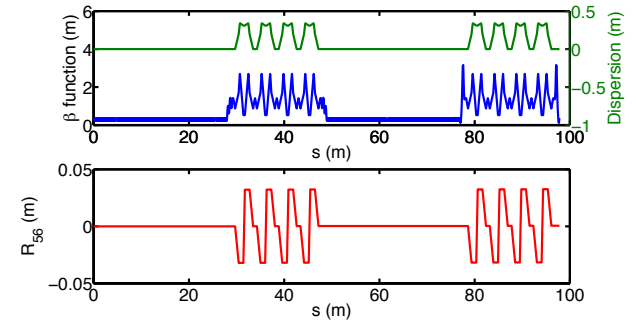

Figure 2: Twiss and momentum compaction functions along the beamline.
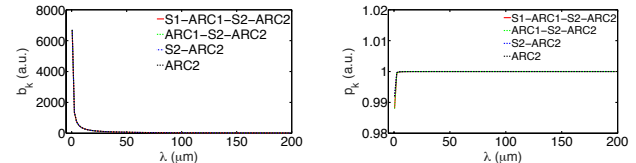

Figure 3: Density (left) and energy (right) modulation spectra for pure optics. Both initial density and energy modulations are included at the beginning.

In particle tracking, such *correlation* information resides in the 4-D/6-D beam phase-space distributions at the exits of every subsections of the beamline. For

05 Beam Dynamics and Electromagnetic Fields

D06 Coherent and Incoherent Instabilities - Measurements and Countermeasures

qualitative comparison, let us consider the two cases in particle tracking: (i) start-to-end tracking (S1-ARC1-S2-ARC2); (ii) S2-ARC2 with initial longitudinal phase-space conditions deduced from those of (i) at the exit of ARC1 while the initial transverse phase-space distribution is set as that of pure optics at the exit of ARC1. Note that Case (ii) would be different from Case (i) in that the transverse-longitudinal correlation has been neglected. To be consistent, only steady-state CSR is included in the tracking simulation. For Case (i), we assume 5% initial energy modulation at 100 μm in the particle tracking. For the latter case, to obtain the initial conditions, we need to identify Twiss functions at the exit of ARC1 to characterize the transverse phase-space distribution but retain the longitudinal phase-space distribution of Case (i) as input at this particular position.
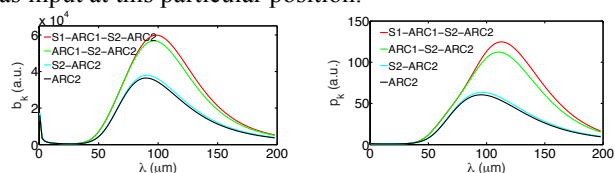

Figure 4: Density (left) and energy (right) modulation spectra including CSR effect.
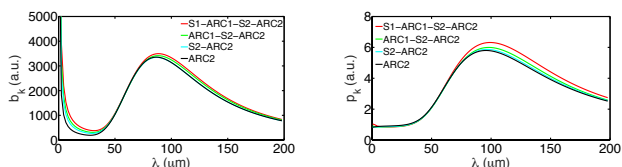

Figure 5: Density (left) and energy (right) modulation spectra with CSR excluded in ARC1.

Figure 6 compares the phase space and current density distributions for both cases at the end of the beamline. The obvious difference has qualitatively confirmed our Vlasov results; both the density and energy modulations from the start-to-end (S1-ARC1-S2-ARC2) case are larger than those starting from midway (S2-ARC) [14].
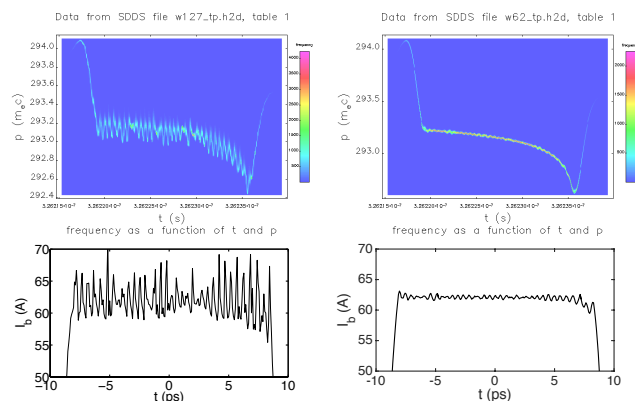

Figure 6: (Top) the longitudinal phase-space distributions at the end of the beamline for Case (i) (left) and Case (ii) (right); (bottom) the bunch current profile for case (i) (left) and (ii) (right).

For further investigation of where the difference originates, it was found a microbunching structure resides

in (x',z) at the exits of ARC1 and of the beamline, as shown in Fig. 7. Indeed such structure is not included in the existing microbunching analysis. Further investigation is under way. This will be the subject of our next study.
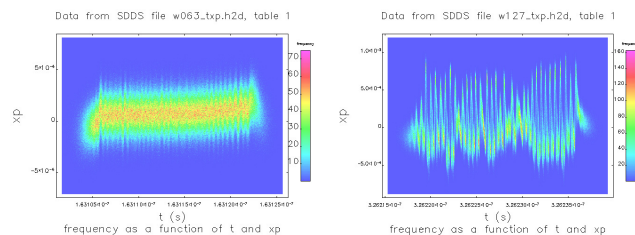

Figure 7: The microbunching structure in (x',t) at the exit of ARC1 (left) and at the end of the beamline (right).

To end this section, we consider a simple case with only initial density modulation. The microbunching gains evaluated from different concatenations are compared with the naïve multiplicative approach, shown in Fig. 8. It appears that the naïve approach gives an underestimate to the overall microbunching gain along the beamline.
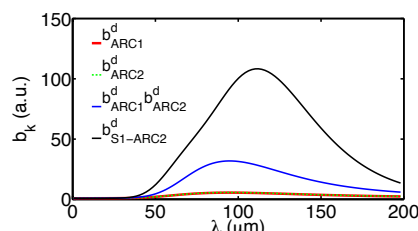

Figure 8: Density modulation spectra based on different considerations (with CSR included).

SUMMARY AND DISCUSSION

In this paper we have already extended the existing single-pass microbunching analysis from density to density modulation to the combination of both density and energy modulations throughout a beamline. The generalized formulation enables us to gain more understanding of the microbunching development along a beamline transport system. Our investigation of a particular recirculating machine indicates that the multiplication of gains from separate sub-beamline sections may underestimate the overall microbunching effect. This is because this way only takes into account the information of longitudinal density and energy modulations, while neglects the correlated structure residing in other dimensions. Such structure might trickle into other dimensions later downstream the beamline [15], e.g. back to (z, δ), as shown in Fig. 6. It can be seen that a more thorough description including the transverse microbunching, as well as the structure residing in the transverse-longitudinal (x, z) or (x', z) dimension, shall be required for more complete analysis.

REFERENCES

[1] C. -Y. Tsai *et al*., Linear Vlasov Solver Microbunching Gain Estimation with Inclusion of CSR, LSC and Linac Geometric Impedances, FEL'15 (MOP052)

[2] S. Heifets *et al*., Coherent synchrotron radiation instability in a bunch compressor, Phys. Rev. ST Accel. Beams 5, 064401 (2002)

[3] Z. Huang and K. Kim, Formulas for coherent synchrotron radiation microbunching in a bunch compressor chicane, Phys. Rev. ST Accel. Beams 5, 074401 (2002)

[4] M. Vneturini, Microbunching instability in a single-pass ystem using a direct two-dimensional Vlasov solver, Phys. Rev. ST Accel. Beams 10, 104401 (2007)

[5] M. Borland, elegant: A Flexible SDDS-Compliant Code for Accelerator Simulation, APS Report No. LS-287, 2000

[6] G. Stupakov and S. Heifets, Beam instability and microbunching due to coherent synchrotron radiation, Phys. Rev. ST Accel. Beams 5, 054402 (2002)

[7] See, for example, Y. Cai, Linear theory of microwave instability in electron storage rings, Phys. Rev. ST Accel. Beams 14, 061002 (2011)

[8] Z. Huang *et al*., Theory and simulation of CSR microbunching in bunch compressors, SLAC-PUB-9538 (2002)

[9] R. Bosch *et al*., Multistage gain of the microbunching instability, FEL'10 (WEPB49)

[10] S. Di Mitri, Intrabeam scattering in high brightness electron linacs, Phys. Rev. ST Accel. Beams 17, 074401 (2014)

[11] D. Douglas *et al*., Control of coherent synchrotron radiation and microbunching effects during transport of high brightness electron beams, arXiv: 1403.2318v1 [physics.acc-ph] and D. Douglas et al., Control of synchrotron radiation effects during recirculation, IPAC'15 (TUPMA038)

[12] Y.S. Derbenev *et al*., Microbunch Radiative Tail-head Interaction, TESLA-FEL 95-05, 1995

[13] J. Murphy *et al*., Longitudinal wakefield for an electron moving on a circular orbit, Part. Accel. 1997, Vol. 57, pp. 9-64

[14] In Fig. 7, it can be seen that the left figure features higher harmonic components, which violate an assumption of the above formulation. It occurs when the microbunching gain is large. Even so, it can be considered qualitatively consistent to our Vlasov analysis.

[15] Z. Huang *et al*., Measurements of the linac coherent light source laser heater and its impact on the x-ray free-electron laser performance, Phys. Rev. ST Accel. Beams 13, 020703 (2010)